# Genetic rescue of lineage-balanced blood cell production reveals a crucial role for STAT3 antiinflammatory activity in hematopoiesis

Huiyuan Zhang[a,1], Haiyan S. Li[a], Emily J. Hillmer[a], Yang Zhao[b], Taylor T. Chrisikos[a,c], Hongbo Hu[a,1], Xiao Wu[d], Erika J. Thompson[d], Karen Clise-Dwyer[e], Karen A. Millerchip[a], Yue Wei[f], Nahum Puebla-Osorio[g], Saakshi Kaushik[h], Margarida A. Santos[h], Bin Wang[d], Guillermo Garcia-Manero[f], Jing Wang[b], Shao-Cong Sun[a,c], and Stephanie S. Watowich[a,c,2]

[a]Department of Immunology, University of Texas MD Anderson Cancer Center, Houston, TX 77030; [b]Department of Bioinformatics and Computational Biology, University of Texas MD Anderson Cancer Center, Houston, TX 77030; [c]The University of Texas Graduate School of Biomedical Sciences, Houston, TX 77030; [d]Department of Genetics, University of Texas MD Anderson Cancer Center, Houston, TX 77030; [e]Department of Stem Cell Transplantation Research, University of Texas MD Anderson Cancer Center, Houston, TX 77030; [f]Department of Leukemia, University of Texas MD Anderson Cancer Center, Houston, TX 77030; [g]Department of Lymphoma and Myeloma, University of Texas MD Anderson Cancer Center, Houston, TX 77030; and [h]Department of Epigenetics and Molecular Carcinogenesis, University of Texas MD Anderson Cancer Center, Houston, TX 77030

Edited by George R. Stark, Lerner Research Institute, The Cleveland Clinic Foundation, Cleveland, OH, and approved January 26, 2018 (received for review August 6, 2017)

**Blood cell formation must be appropriately maintained throughout life to provide robust immune function, hemostasis, and oxygen delivery to tissues, and to prevent disorders that result from over- or underproduction of critical lineages. Persistent inflammation deregulates hematopoiesis by damaging hematopoietic stem and progenitor cells (HSPCs), leading to elevated myeloid cell output and eventual bone marrow failure. Nonetheless, antiinflammatory mechanisms that protect the hematopoietic system are understudied. The transcriptional regulator STAT3 has myriad roles in HSPC-derived populations and nonhematopoietic tissues, including a potent antiinflammatory function in differentiated myeloid cells. STAT3 antiinflammatory activity is facilitated by STAT3-mediated transcriptional repression of *Ube2n*, which encodes the E2 ubiquitin-conjugating enzyme Ubc13 involved in proinflammatory signaling. Here we demonstrate a crucial role for STAT3 antiinflammatory activity in preservation of HSPCs and lineage-balanced hematopoiesis. Conditional *Stat3* removal from the hematopoietic system led to depletion of the bone marrow lineage$^-$ Sca-1$^+$ c-Kit$^+$ CD150$^+$ CD48$^-$ HSPC subset (LSK CD150$^+$ CD48$^-$ cells), myeloid-skewed hematopoiesis, and accrual of DNA damage in HSPCs. These responses were accompanied by intrinsic transcriptional alterations in HSPCs, including deregulation of inflammatory, survival and developmental pathways. Concomitant *Ube2n*/Ubc13 deletion from *Stat3*-deficient hematopoietic cells enabled lineage-balanced hematopoiesis, mitigated depletion of bone marrow LSK CD150$^+$ CD48$^-$ cells, alleviated HSPC DNA damage, and corrected a majority of aberrant transcriptional responses. These results indicate an intrinsic protective role for STAT3 in the hematopoietic system, and suggest that this is mediated by STAT3-dependent restraint of excessive proinflammatory signaling via Ubc13 modulation.**

STAT3 | hematopoiesis | inflammation | Ubc13

Hematopoietic stem cells (HSCs) and multipotent progenitors (collectively termed HSPCs) generate the full repertoire of myeloid and lymphoid populations in homeostasis, and respond to physiological stress, such as infection, by tailoring a hematopoietic response needed to resolve the insult. Hence, understanding mechanisms that preserve HSPC function is important for insight into the dynamic nature and long-term maintenance of the hematopoietic system. Recent work has shown that inflammatory cytokines produced during bacterial or viral infections transiently influence HSPC activity, while persistent inflammation degrades HSPCs and can lead to failure of hematopoiesis (1–5). During chronic inflammation, HSPCs show increased proliferation, accumulation of DNA damage, myeloid-skewing, and impaired repopulating activity (5–9). Chronic inflammation and genetic deregulation of inflammatory mediators is also associated with myelodysplastic syndrome and acute myeloid leukemia in humans (10–16). Furthermore, it is increasingly clear that certain cancers remodel hematopoiesis via tumor-derived inflammatory factors, with deleterious effects on tumor immunity (17–19). Despite clear links between inflammation, HSPC injury, and hematopoietic imbalance, there is little understanding of underlying molecular pathways or protective mechanisms that mitigate inflammation-induced damage.

The transcriptional regulator STAT3 is a critical signaling intermediate for multiple cytokines and growth factors; studies in animal models have delineated important biological activities of STAT3 in many immune populations and nonimmune tissues

## Significance

**Inflammation degrades hematopoietic stem and progenitor (HSPC) function, leading to myeloid-skewing and bone marrow failure. We show that the transcriptional regulator STAT3 has an intrinsic protective role in the hematopoietic system, which is necessary to preserve HSPCs and lineage-balanced hematopoiesis. We find that concomitant removal of *Ube2n*, encoding the proinflammatory signal transducer Ubc13, mitigates hematopoietic failure, myeloid overproduction, and a majority of transcriptional deregulation within *Stat3*-null HSPCs. These data imply an epistatic relationship between *Stat3* and *Ube2n*, and suggest that STAT3 protects the hematopoietic system from the effects of excessive proinflammatory signaling by restraining Ubc13.**

Author contributions: H.Z., H.S.L., E.J.H., X.W., E.J.T., K.A.M., M.A.S., B.W., and S.S.W. designed research; H.Z., H.S.L., E.J.H., Y.Z., T.T.C., H.H., X.W., E.J.T., K.C.-D., K.A.M., N.P.-O., S.K., J.W., and S.S.W. performed research; S.-C.S. contributed new reagents/analytic tools; H.Z., H.S.L., E.J.H., Y.Z., T.T.C., X.W., K.C.-D., Y.W., N.P.-O., S.K., M.A.S., B.W., G.G.-M., J.W., S.-C.S., and S.S.W. analyzed data; and S.S.W. wrote the paper.

The authors declare no conflict of interest.

This article is a PNAS Direct Submission.



Data deposition: Sequencing data were deposited in the NCBI Sequence Read Archive (accession no. PRJNA363078).

[1]Present address: Department of Rheumatology and Immunology, State Key Laboratory of Biotherapy and Collaborative Innovation Center for Biotherapy, West China Hospital, Sichuan University, 610041 Chengdu, China.

[2]To whom correspondence should be addressed. Email: swatowic@mdanderson.org.

This article contains supporting information online at www.pnas.org/lookup/suppl/doi:10.1073/pnas.1713889115/-/DCSupplemental.

Published online February 20, 2018.

(20–22). Moreover, aberrant STAT3 activity promotes diseases, such as cancer or immune deregulation. For example, loss-of-function (LOF) or gain-of-function (GOF) *STAT3* mutations in humans associate with immunodeficiency or autoimmunity, respectively (23–26), while persistent STAT3 signaling is a feature of malignant cell growth as well as tumor-mediated immune suppression (27, 28). Although STAT3 therapeutics are under development (29, 30), further work is necessary to understand fundamental roles of STAT3 in vivo and thus provide new approaches to manage diseases with *STAT3* mutations, as well as cancers and inflammatory disorders associated with sustained STAT3 activation.

In the process of hematopoiesis, STAT3 controls proliferation of defined progenitor subsets in response to cytokines that rely on this factor as a principal signal transducer. For example, STAT3 is required for granulocyte-colony stimulating-factor (G-CSF) –dependent proliferation of granulocyte-monocyte progenitors (GMPs), and Fms-related tyrosine kinase 3 ligand (Flt3L)-mediated growth of $Flt3^+$ dendritic cell progenitors (31, 32). The repopulating function of total bone marrow or fetal liver cells also requires transcriptionally active STAT3 (33, 34); transplantation of *Stat3*-deficient bone marrow cells leads to myeloid-skewed hematopoiesis and peripheral myeloid accumulation (35). Moreover, recent work indicated that homeostatic maintenance of HSPCs is dependent upon functional STAT3. Mice with hematopoietic and endothelial *Stat3* deletion show reduced amounts of $CD34^-$ $lineage^-$ ($lin^-$) Sca-$1^+$ c-$Kit^+$ cells in bone marrow (36); this phenotypically defined subset includes long-term repopulating HSCs. Consistently, the total bone marrow population from these animals showed defective repopulating activity in lethally irradiated recipients (36). These studies indicate STAT3 is important for maintaining HSPC amounts, bone marrow reconstitution, and lineage-balanced hematopoiesis, yet the underlying mechanisms by which these functions are accomplished remain unresolved.

In contrast, experiments with mature myeloid cells revealed a potent antiinflammatory role for STAT3. This function is demonstrated by STAT3-mediated restraint of Toll-like receptor 4 (TLR4) -induced proinflammatory cytokine and chemokine gene expression (37–40). Myeloid cells lacking STAT3 have elevated TLR4 signaling, culminating in overproduction of proinflammatory factors, such as TNF-α and IFN-γ. The hyperactive myeloid response drives a lethal type I inflammatory disease in mice with STAT3-deficiency in hematopoietic and endothelial cells, or the myeloid lineages, by early adulthood (35, 37, 41). *STAT3* LOF mutations in humans are accompanied by disordered inflammation, suggesting that STAT3 antiinflammatory function is conserved (23, 42). Recently, we found STAT3 restrains proinflammatory signals by acting as a transcriptional repressor on *Ube2n*, which encodes Ubc13, a key component of TLR signaling cascades leading to proinflammatory cytokine gene activation (40, 43). Myeloid cells with *Stat3*-deficiency accumulate Ubc13 due to failure to suppress *Ube2n* transcription, and elevated Ubc13 protein is necessary for inducing excessive proinflammatory gene-expression responses in *Stat3*-deficient cells upon TLR4 ligation (40). While these data indicate that the molecular basis of the STAT3 antiinflammatory response is mediated by modulation of Ubc13, the impact of this signaling pathway in vivo remains unclear.

Collectively, prior work has linked inflammation with HSPC deregulation. Previous studies have also indicated key associations between STAT3 and inflammation restraint, as well as STAT3 and hematopoietic function. Nonetheless, it remains unclear whether hematopoietic-intrinsic STAT3 function and STAT3 antiinflammatory activity are important in hematopoiesis. In this study, we use several genetic models and transcriptional profiling of HSPCs to examine the role of STAT3 in protection of hematopoiesis.

## Results

**HSPC Failure in Tie2 Cre *Stat3$^{f/f}$* Mice.** Prior studies examining STAT3 function in hematopoiesis showed defective repopulating activity of total bone marrow from animals with *Stat3*-deficiency (Tie2 cre *Stat3$^{f/f}$* mice) (36). Nonetheless, it remained unclear whether impaired repopulation was a consequence of fewer HSPCs or defective HSPC function, because HSPC amounts were reduced in these animals (36). Using a distinct phenotypic analysis for HSPCs, we found a substantial reduction in the absolute number and proportion of LSK $CD150^+$ $CD48^-$ cells, a population enriched for long-term repopulating HSCs (44), within Tie2 cre *Stat3$^{f/f}$* mice versus controls (Fig. 1 *A* and *B*; see Fig. S1 *A* and *B* for gating and analysis strategies). We next tested whether the LSK $CD150^+$ $CD48^-$ cells remaining in Tie2 cre *Stat3$^{f/f}$* mice were functional by performing transplantation experiments. Using FACS, we purified 200 LSK $CD150^+$ $CD48^-$ cells from Tie2 cre *Stat3$^{f/f}$* mice or controls (both $CD45.2^+$), and transferred these cells into lethally irradiated congenic $CD45.1^+$ recipients in conjunction with a radioprotective dose of recipient bone marrow (Fig. 1*C*). By transplanting similar numbers of purified HSPCs from each genotype, we were able to circumvent defects in their amounts and track their function directly via reconstitution of $CD45.2^+$ cells in peripheral blood. These assays revealed a marked inability of LSK $CD150^+$ $CD48^-$ cells from Tie2 cre *Stat3$^{f/f}$* mice to reconstitute hematopoiesis, as judged by an almost complete failure to repopulate peripheral blood (Fig. 1*D*). These data indicate that STAT3 is critical for maintaining HSPC numbers and HSPC repopulating function in vivo.

To probe mechanisms leading to the HSPC functional defect, we examined cell cycle status. Infrequent cell cycling, or a quiescent state, is critical for long-term HSC activity, multilineage hematopoiesis, and protection from exhaustion (45, 46). We detected a significant increase in the $K_i67^+$ $Hoechst^{lo}$ (G1) population within the bone marrow LSK $CD150^+$ $CD48^-$ subset and the total LSK fraction of Tie2 cre *Stat3$^{f/f}$* mice, relative to *Stat3*-sufficient controls. This was accompanied by a corresponding decrease in the $K_i67^-$ $Hoechst^{lo}$ (G0) subset (Fig. 2 *A*–*D*). These data show a greater percentage of *Stat3*-deficient LSK $CD150^+$ $CD48^-$ cells and LSKs are in G1 vs. G0, implying increased cell cycling. Significantly, previous work has demonstrated LSK amounts are either increased or unaffected in Tie2 cre *Stat3$^{f/f}$* mice (31, 36), suggesting augmented cell cycle activity selectively impacts maintenance of the LSK $CD150^+$ $CD48^-$ subset.

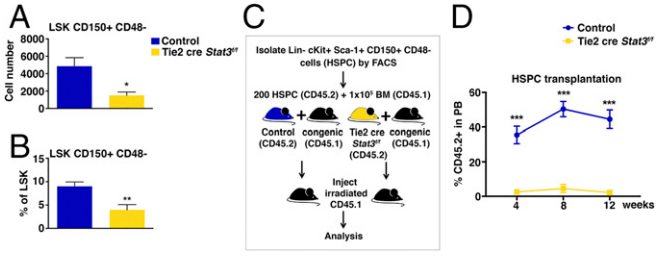


**Fig. 1.** Abundance and function of HSPCs in Tie2 cre *Stat3$^{f/f}$* mice. (*A* and *B*) Mean values of cumulative LSK $CD150^+$ $CD48^-$ cell numbers (*A*) and frequencies (within LSK compartment) (*B*) in Tie2 cre *Stat3$^{f/f}$* (yellow bars) and *Stat3*-sufficient controls (blue bars). $n = 4$ per genotype, four independent experiments. (*C*) Schematic of transplantation assay using purified donor LSK $CD150^+$ $CD48^-$ cells. (*D*) Hematopoietic reconstitution activity of donor LSK $CD150^+$ $CD48^-$ cells, assessed by measuring the abundance of circulating $CD45.2^+$ cells at 4-wk intervals (4–12 wk) after transplantation. Data represent mean values of $n = 10$ per genotype, two independent experiments. (*A*, *B*, and *D*) Data were analyzed by Student's *t* test (*A* and *B*), or two-way ANOVA with multiple comparisons, comparing control and Tie2 cre *Stat3$^{f/f}$* at each time point (*D*). $*P < 0.05$; $**P < 0.01$; $***P < 0.001$ for indicated comparisons. Error bars indicate SEM.

Excessive proliferation has been linked with accumulation of DNA damage in HSPCs (8). Consistently, LSKs from Tie2 cre *Stat3*$^{f/f}$ mice exhibited increased DNA damage, as judged by elevated amounts of phosphorylated H2AX (γH2AX) compared with controls (Fig. 2 *E* and *F*). These results were confirmed by alkaline comet assays (Fig. 2*G* and Fig. S1*C*). A trend toward increased γH2AX was also found in LSK CD150$^+$ CD48$^-$ cells from Tie2 cre *Stat3*$^{f/f}$ mice, although this did not reach statistical significance (Fig. S1 *D* and *E*). Collectively, the observations of increased cell cycling and DNA damage suggested severe injuries within the *Stat3*-deficient LSK compartment, as well as the few LSK CD150$^+$ CD48$^-$ HSPCs remaining in Tie2 cre *Stat3*$^{f/f}$ mice.

**Functional HSPCs in Mice with Myeloid-Restricted *Stat3*-Deficiency.** Tie2 cre *Stat3*$^{f/f}$ mice lack STAT3 throughout all stages of hematopoietic development. By 4–6 wk of age, these animals exhibit enterocolitis, increased blood and tissue-infiltrating myeloid cells, myeloid hyperreactivity to TLR2/4 agonists, and elevated peripheral type I proinflammatory cytokines (e.g., TNF-α, IFN-γ), causing lethality in young adulthood (35, 41). Furthermore, the Tie2 cre transgene mediates deletion of floxed alleles in endothelial cells (47), which comprise an important HSC niche population (48, 49). Thus, the HSPC defects observed in Tie2 cre *Stat3*$^{f/f}$ mice could result from peripheral inflammatory disease, deficiencies in the bone marrow niche, an intrinsic requirement for STAT3 in HSPCs, or a combination of these effects. Therefore, we utilized distinct animal models to delineate STAT3 roles in hematopoiesis.

To distinguish between peripheral inflammatory disease driven by *Stat3*-deficiency and an intrinsic role for STAT3 in HSPCs, we employed the LysM cre *Stat3*$^{f/f}$ model. These animals develop an inflammatory syndrome similar to Tie2 cre *Stat3*$^{f/f}$ mice due to hyperactive myeloid cells, yet STAT3 is retained within the HSPC compartment (37). We found diseased LysM cre *Stat3*$^{f/f}$ animals and age-matched, nondiseased controls had comparable proportions of LSK CD150$^+$ CD48$^-$ cells in bone marrow (Fig. S2 *A* and *B*). Moreover, the repopulating activity of LSK CD150$^+$ CD48$^-$ cells purified from diseased LysM cre *Stat3*$^{f/f}$ animals was indistinguishable from controls, as judged by their contribution to peripheral blood in congenic CD45.1$^+$ recipients (Fig. S2*C*). We also observed a similar abundance of donor-derived CD45.2$^+$ LSKs and CD45.2$^+$ LSK CD150$^+$ CD48$^-$ cells in both cohorts of recipient mice 20 wk after transplantation (Fig. S2 *D* and *E*), suggesting long-term HSPC reconstitution was equivalent between genotypes. Together, these data indicate the extent and duration of peripheral, myeloid-mediated type I inflammation in LysM cre *Stat3*$^{f/f}$ animals is not sufficient to decrease amounts or deregulate activity of HSPCs with intact STAT3.

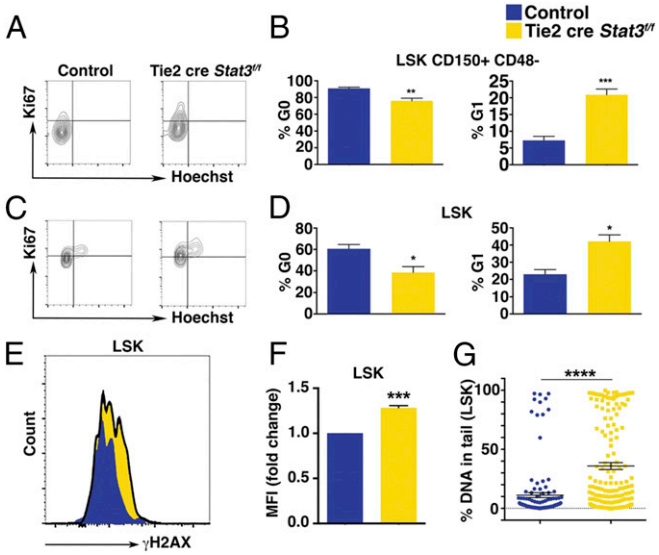


**Fig. 2.** Phenotype of HSPCs in Tie2 cre *Stat3*$^{f/f}$ mice. (*A*–*D*) Representative (*A* and *C*) and cumulative mean values (*B* and *D*) from cell cycle analysis of LSK CD150$^+$ CD48$^-$ cells (*A* and *B*) and LSKs (*C* and *D*) in Tie2 cre *Stat3*$^{f/f}$ (yellow bars) and *Stat3*-sufficient mice (blue bars), as indicated. $n = 3$ per genotype, three independent experiments. (*E*) Representative results showing γH2AX abundance in LSKs from Tie2 cre *Stat3*$^{f/f}$ and *Stat3*-sufficient mice. Results represent one of three independent experiments. (*F*) Cumulative results of γH2AX analysis of LSKs from Tie2 cre *Stat3*$^{f/f}$ and *Stat3*-sufficient mice. Data are shown as means of mean fluorescence intensity (MFI); Tie2 cre *Stat3*$^{f/f}$ results normalized to *Stat3*-sufficient control. $n = 3$ per genotype, three independent experiments. (*G*) Cumulative results of alkaline comet assay analysis of LSKs purified from Tie2 cre *Stat3*$^{f/f}$ and *Stat3*-sufficient mice. More than 100 cells analyzed per genotype, $n = 2$ per genotype, representative of two independent experiments. (*B*, *D*, *F*, and *G*) Data were analyzed by Student's *t* test, comparing control and Tie2 cre *Stat3*$^{f/f}$. *$P < 0.05$; **$P < 0.01$; ***$P < 0.001$; ****$P < 0.0001$ for indicated comparisons. Error bars indicate SEM.

**Intrinsic Role for *Stat3* in the Hematopoietic System.** The impaired function of HSPCs from Tie2 cre *Stat3*$^{f/f}$ mice versus the lack of obvious defects in HSPCs from LysM cre *Stat3*$^{f/f}$ animals suggested a cell-autonomous role for STAT3 in HSPC regulation. Nonetheless, Tie2 cre also deletes from endothelial cells, which are important for HSC maintenance (47–49). This raised the question of whether HSPC deregulation in Tie2 cre *Stat3*$^{f/f}$ mice resulted from hematopoietic or nonhematopoietic STAT3 function. Accordingly, we developed a model to test the hematopoietic activity of STAT3 exclusively, allowing us to circumvent effects of *Stat3* deletion from nonhematopoietic cells. We generated CreER *Stat3*$^{f/f}$ mice, which contain a tamoxifen-inducible cre isoform produced ubiquitously under control of the *Rosa26* promoter (50). We next established bone marrow chimeras to limit cre activity to the hematopoietic system, by transplanting bone marrow cells from CreER *Stat3*$^{f/f}$ mice or *Stat3*$^{f/f}$ controls (CD45.2$^+$) into lethally irradiated congenic CD45.1$^+$ recipients (Fig. S3*A*). Importantly, bone marrow from both donors demonstrated similar reconstitution (>80%), as judged by analysis of donor-derived peripheral blood CD45.2$^+$ cells at 6–8 wk following transplantation (Fig. S3*B*, time 0). We then stimulated cre activity by tamoxifen administration to induce *Stat3* deletion, and confirmed effective STAT3 depletion in hematopoietic cells of CreER *Stat3*$^{f/f}$ chimeras versus controls (Fig. S3*C*). While *Stat3*-deficient chimeras initially showed hematopoietic activity comparable to controls, we observed a significant decrease in circulating CD45.2$^+$ cells in animals with *Stat3*-deficient bone marrow by 20 wk after gene deletion (Fig. S3*B*), indicating STAT3 has an intrinsic role in the hematopoietic system to maintain effective blood cell production.

Failure of hematopoiesis, excessive HSPC proliferation, and DNA damage are hallmarks of HSPC responses to inflammation. Prior studies have shown HSPCs directly sense TLR agonists and respond by production of classic proinflammatory cytokines (51–53). To test whether STAT3 exerted antiinflammatory activity in HSPCs, LSKs were purified from tamoxifen-treated CreER *Stat3*$^{f/f}$ and control *Stat3*$^{f/f}$ mice, and stimulated ex vivo with a TLR2 agonist (Pam3CSK4). These assays revealed elevated proinflammatory gene expression in *Stat3*-deficient LSKs upon Pam3CSK4 treatment, relative to controls (Fig. S3*D*). Basal expression of proinflammatory genes, such as *Ifnb* and *Il6*, was also increased in *Stat3*-deficient LSKs (Fig. S3*D*). These data indicate intrinsic antiinflammatory activity for STAT3 within the HSPC compartment.

**Requirement for *Ube2n* in Hematopoietic Failure and Myeloid-Skewing with *Stat3*-Deficiency.** The antiinflammatory activity of STAT3 in mature myeloid cells is mediated by STAT3-dependent transcriptional repression of *Ube2n*, encoding the E2 ubiquitin-conjugating enzyme Ubc13, a central mediator of proinflammatory signaling and gene expression upon TLR stimulation (40, 43). We hypothesized

STAT3 protects hematopoiesis via a similar pathway, and envisaged *Ube2n* deletion from *Stat3*-deficient hematopoietic cells would restore HSPC amounts and hematopoietic function. To test this, we generated CreER *Stat3*$^{f/f}$ mice containing a conditional *Ube2n* allele (i.e., CreER *Stat3*$^{f/f}$ *Ube2n*$^{f/f}$ animals), along with relevant control strains (all CD45.2$^+$). We then established bone marrow chimeric mice using these strains as donors, with transplantation into lethally irradiated congenic CD45.1$^+$ recipients (Fig. 3*A*). This approach allowed us to stimulate hematopoietic-restricted deletion of *Stat3*, *Ube2n*, or *Stat3* and *Ube2n* simultaneously, using tamoxifen treatment (Fig. 3*A*). Significantly, bone marrow from all four strains engrafted with similar ability and demonstrated comparable lineage reconstitution before tamoxifen delivery (Fig. 3 *B* and *C*, time 0). Upon inducible gene deletion, we observed effective reduction of STAT3 and Ubc13 in bone marrow cells from relevant chimeric mice (Fig. S4*A*).

We confirmed loss of hematopoietic activity upon *Stat3* deletion (Fig. 3*B* and Fig. S4*B*). Moreover, we found significant myeloid-skewed hematopoiesis resulting from hematopoietic-restricted *Stat3*-deficiency. This was evidenced by an approximate threefold increase in circulating donor-derived CD45.2$^+$ CD11b$^+$ myeloid cells at 8 wk following *Stat3* removal, and a seven- to eightfold increase by 20 wk, compared with all other cohorts (Fig. 3*C*, *Left*), as well as reduction in peripheral blood CD45.2$^+$ B220$^+$ B lymphocyte and CD45.2$^+$ CD3$^+$ T lymphocyte populations at 20 wk after gene deletion (Fig. 3*C*, *Center* and *Right*). Myeloid-skewed hematopoiesis in *Stat3*-deficient chimeras was accompanied by elevated amounts of circulating proinflammatory cytokines (Fig. 3*D*). Recipient-origin myeloid cells were not elevated in mice with hematopoietic *Stat3*-deficiency (Fig. S4*B*), suggesting myeloid accumulation is intrinsic to *Stat3*-deficient cells. Furthermore, *Ube2n* deletion alone did not alter circulating T or B cell amounts appreciably (Fig. 3*C*, *Center* and *Right*).

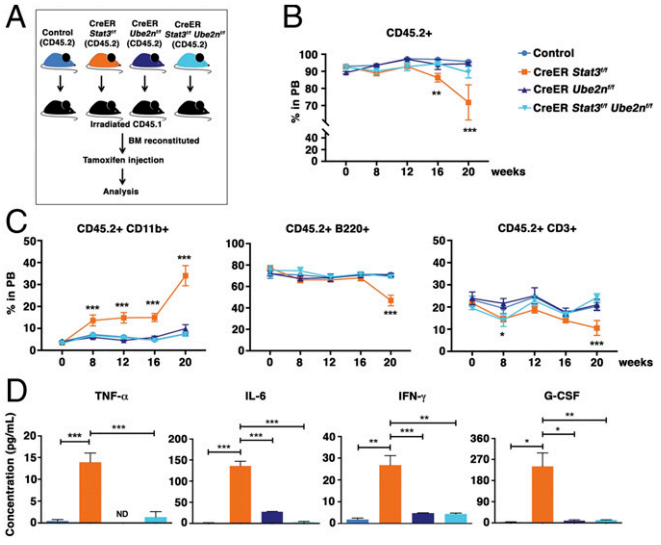


**Fig. 3.** Hematopoietic-intrinsic roles for STAT3 and Ubc13 in peripheral blood reconstitution. (*A*) Schematic diagram of the experimental approach to generate chimeric mice containing *Stat3*- *Ube2n*-sufficient (control; medium blue), *Stat3*-deficient (orange), *Ube2n*-deficient (purple), or *Stat3*- *Ube2n*-deficient (aqua) hematopoietic compartments. (*B*) Contribution of donor bone marrow to peripheral blood (PB), evaluated by measuring circulating CD45.2$^+$ cells before tamoxifen delivery (0) and at 4-wk intervals following tamoxifen treatment, as shown. (*C*) Reconstitution of myeloid and lymphoid lineages, determined by measuring the proportion of circulating CD45.2$^+$ CD11b$^+$ (myeloid), CD45.2$^+$ B220$^+$ (B lymphocytes), and CD45.2$^+$ CD3$^+$ (T lymphocytes) before tamoxifen delivery (0) and at 4-wk intervals following tamoxifen treatment, as shown. (*B* and *C*) $n$ = 8–10 per genotype. Results represent one of three independent experiments. (*D*) Cytokine profiles in serum collected from bone marrow chimeric mice, 20 wk posttamoxifen treatment. $n$ = 3 per genotype. (*B–D*) Data analyzed by two-way ANOVA with multiple comparisons (*B* and *C*; comparing time points within each group), or one-way ANOVA with multiple comparisons (*D*). *$P$ < 0.05; **$P$ < 0.01; ***$P$ < 0.001 for indicated comparisons. Error bars indicate SEM.

Notably, simultaneous *Stat3* and *Ube2n* removal resulted in effective contribution to peripheral blood, with activity indistinguishable from *Stat3*- *Ube2n*-sufficient controls or the *Ube2n*-deficient cohort (Fig. 3*B*). Concomitant removal of *Stat3* and *Ube2n* also suppressed myeloid-skewing and circulating proinflammatory cytokine amounts (Fig. 3 *C* and *D*). Taken together, our data indicate hematopoietic-intrinsic STAT3 function is required for lineage-balanced blood cell production, and Ubc13 expression is central to hematopoietic failure with *Stat3*-deficiency.

To evaluate this further, we measured amounts of donor-derived hematopoietic progenitors in the bone marrow of chimeric mice 20 wk following gene deletion, at which point animals with hematopoietic *Stat3*-deficiency exhibited significant increases in circulating myeloid cells and proinflammatory cytokines (Fig. 3 *C* and *D*). We found elevated amounts (~threefold) of donor-derived CD45.2$^+$ GMPs, accompanied by a substantial reduction in CD45.2$^+$ common myeloid (CMP) and megakaryocyte-erythroid (MEP) progenitor populations, in *Stat3*-deficient mice vs. controls (Fig. 4 *A* and *B*). Donor-origin progenitor amounts in chimeras with concomitant *Stat3* and *Ube2n* deletion were similar to controls, consistent with observations of peripheral blood lineages (Figs. 3 and 4 *A* and *B*). Progenitor amounts were largely unaffected by *Ube2n* deletion alone, with the exception of an increase in CMPs (Fig. 4 *A* and *B*). In addition, the frequency of donor-origin CD45.2$^+$ LSKs, as well as CD45.2$^+$ lin$^-$ Sca-1$^-$ c-Kit$^+$ cells, a population enriched for myeloid progenitors, was comparable among all groups (Fig. S4 *C* and *D*). Our results show hematopoietic-intrinsic STAT3 function is critical to maintain committed myeloid progenitor subsets at appropriate ratios, while progenitor deregulation with *Stat3*-deficiency involves Ubc13.

We next assessed whether *Ube2n* removal from *Stat3*-deficient hematopoietic cells affected HSPC responses linked with excessive inflammatory signaling. We observed a substantial accumulation of γH2AX amounts in CD45.2$^+$ *Stat3*-deficient LSKs from bone marrow chimeric mice, which resembled our findings in LSKs from Tie2 cre *Stat3*$^{f/f}$ animals (Figs. 2 *E–G* and 4 *C* and *D*). In contrast, γH2AX amounts were lower in LSKs lacking *Stat3* and *Ube2n*, and were comparable to controls or *Ube2n*-deficient cells (Fig. 4 *C* and *D*). A similar trend was found in the LSK CD150$^+$ CD48$^-$ subset, although these data were not statistically significant (Fig. S4*E*). In addition, we observed a significant decrease in donor-origin HSPCs in animals with hematopoietic-specific *Stat3* deletion, as judged by reduced LSK CD150$^+$ CD48$^-$ cells versus controls (Fig. 4 *E* and *F*). *Ube2n* removal alone showed a trend toward fewer LSK CD150$^+$ CD48$^-$ cells, yet this did not reach statistical significance (Fig. 4 *E* and *F*). Strikingly, the amount of LSK CD150$^+$ CD48$^-$ cells was relatively unaffected upon concomitant deletion of *Stat3* and *Ube2n*, compared with controls, and was increased significantly over *Stat3*-deficient chimeras (Fig. 4 *E* and *F*). These results demonstrate a hematopoietic-intrinsic role for STAT3 in HSPC maintenance and protection from DNA damage by a mechanism involving Ubc13. Collectively, our data suggest STAT3 antiinflammatory activity is critical for HSPC preservation and lineage-balanced hematopoiesis.

**STAT3 and Ubc13 Roles in Hematopoietic Progenitor Transcriptional Responses.** The molecular pathways that are deregulated in HSPCs during inflammation-induced damage are poorly resolved. To better understand these and assess genome-wide transcriptional responses mediated by STAT3 and Ubc13, we performed RNA-sequencing (RNA-seq) studies. Total RNA isolated from donor-derived LSKs (CD45.2$^+$), purified from chimeric mice 20 wk following gene deletion was used for the RNA-seq analysis. This approach allowed us

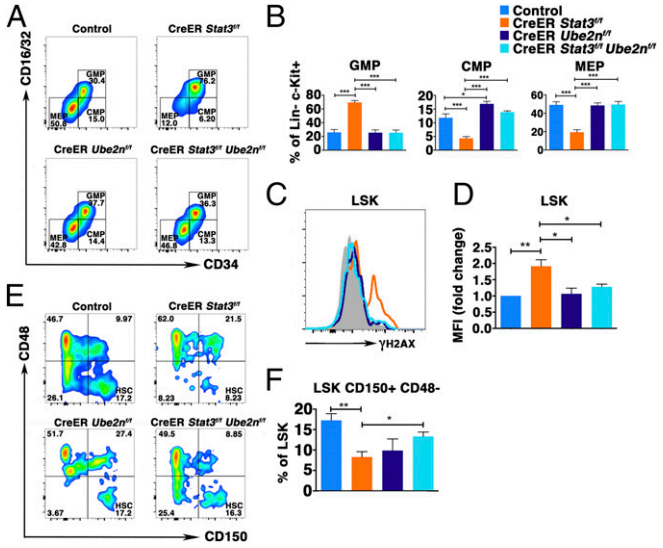


**Fig. 4.** Hematopoietic-intrinsic roles for STAT3 and Ubc13 in regulation of bone marrow progenitor subsets. (*A* and *B*) Representative data (*A*) and cumulative mean values (*B*) of CD45.2$^+$ GMP, CMP, and MEP frequencies in bone marrow chimeric mice, determined 20 wk posttamoxifen treatment. (*C* and *D*) Representative (*C*) and cumulative results (*D*) of γH2AX abundance in purified LSKs from chimeric mice, determined by flow cytometry, as shown. Data are shown as mean MFI, normalized to *Stat3- Ube2n*-sufficient controls (*D*). (*E* and *F*) Representative data (*E*) and cumulative mean values (*F*) of LSK CD150$^+$ CD48$^-$ cell frequencies in chimeric mice, determined at 20 wk posttamoxifen treatment. (*A*–*F*) $n = 3$ per genotype, three independent experiments. (*B*, *D*, and *F*) One-way ANOVA with multiple comparisons used. $^*P < 0.05$; $^{**}P < 0.01$; $^{***}P < 0.001$, for indicated comparisons. Error bars indicate SEM.

to measure global LSK transcriptional responses in *Stat3*-deficient progenitors, which show evidence of inflammation-induced damage, as well as transcriptional patterns in apparently undamaged LSKs from control, *Ube2n*-deficient, or *Stat3- Ube2n*-deficient chimeras (Fig. 4). We confirmed efficient removal of *Stat3* and *Ube2n* in LSKs used for RNA-seq by qPCR analysis (Fig. S5*A*).

Following verification of similar read counts and RNA-seq data quality from all cohorts (Fig. S5*B*), the results were filtered to remove genes with <30 read counts, which eliminated 3,249 genes from further analysis. The remaining 13,083 genes were evaluated by negative binomial generalized linear models followed by likelihood ratio tests, or pairwise comparisons between genotypes using Wald tests. Each pairwise comparison revealed significant gene-expression differences, with the exception of the comparison between control and *Stat3- Ube2n*-deficient LSKs (Fig. S5*C* and Tables S1 and S2), thus implying similarity between the transcriptomes of control LSKs and LSKs lacking both *Stat3* and *Ube2n*. The likelihood ratio tests among all four groups revealed 166 genes with false-discovery rate (FDR) -adjusted q value < 0.01 (Table S3). These differentially expressed genes were displayed in a heatmap, which indicated control and *Stat3- Ube2n*-deficient LSKs show more closely related gene-expression patterns to one another versus the other cohorts (Fig. 5*A*). Using principal component analysis of the 166 genes with FDR-adjusted q value < 0.01, we confirmed a closer relationship between gene-expression in control and *Stat3-Ube2n*-deficient LSKs vs. *Stat3-* or *Ube2n*-deficient LSKs (Fig. S5*D*). Thus, two independent classification approaches showed comparable gene-expression patterns in control and *Stat3-Ube2n*-deficient LSKs, and indicated these are distinct from transcriptional profiles in *Stat3-* or *Ube2n*-deficient LSKs. These data are consistent with the improved hematopoietic function, HSPC amounts, and lack of HSPC DNA damage upon concomitant *Stat3* and *Ube2n* removal, relative to *Stat3*-deficiency alone, as well as similarities between hematopoietic function in *Stat3- Ube2n*-deficient chimeras and *Stat3- Ube2n*-sufficient controls (Figs. 3 and 4).

To evaluate affected cellular responses, we performed a series of pathway analyses on the 166 genes that showed significant differences in expression among the four genotypes (Fig. 5*A* and Table S3). Ingenuity pathway analysis (IPA) indicated deregulation of cancer-related, survival, cellular injury, developmental, and inflammatory pathways upon *Stat3-* or *Ube2n*-deletion in LSKs (Fig. 5 *B* and *C* and Table S4). Comparison analysis of pairwise combinations in IPA revealed opposing or disparate regulation of cell death genes in *Stat3*-deficient vs. *Ube2n*-deficient LSKs, with elevated expression in *Stat3*-deficient LSKs and reduced expression in *Ube2n*-deficient LSKs, upon comparison of each individually to *Stat3- Ube2n*-sufficient controls (Fig. 5*D*). To further understand the impact of this transcriptional deregulation, we analyzed the group of survival genes identified by IPA and found overlap with inflammatory and hematological developmental pathways (Fig. 5 *E* and *F* and Table S4). Using lin$^-$ cells purified from bone marrow chimeric mice, we validated deregulation of 7 of 12 genes tested in

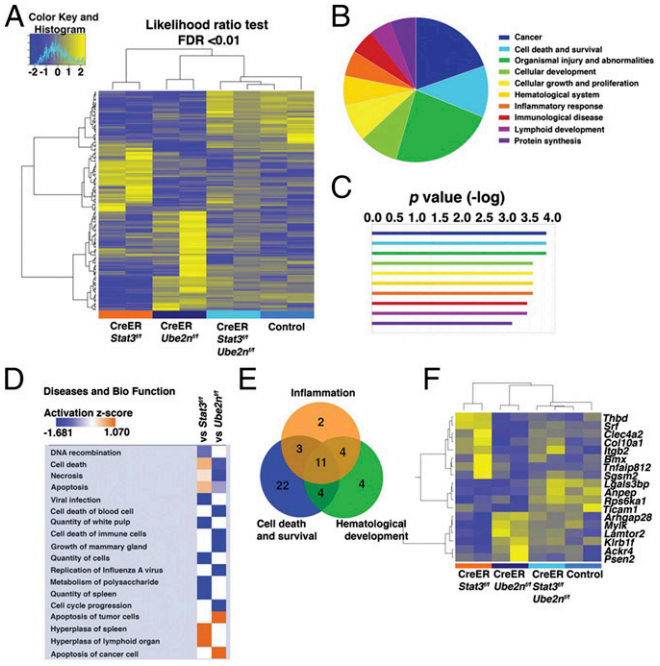


**Fig. 5.** Transcriptome analysis of LSKs with *Stat3-* and *Ube2n*-deficiency. (*A*) Heatmap of genes with significantly different expression in control, *Stat3*-deficient, *Ube2n*-deficient, and *Stat3- Ube2n*-deficient LSKs, determined by negative binomial generalized linear models followed by likelihood ratio tests. The heatmap displays 166 genes with FDR q value < 0.01. Samples and genes were clustered using Pearson distance metric and Ward's minimum variance method. (*B* and *C*) Distribution of 166 genes with FDR q value < 0.01 in the top 10 functional and disease groups, determined by IPA. (*C*) The *P* values (–log) (shown on top row) indicate the likelihood of random association between identified genes and the related functional categories. Larger –log values indicate smaller *P* values, and less chance of random association. $P < 0.05$ generally indicate a statistically significant, nonrandom association. –log = 3 was used to select the top 10 groups, which equals $P < 0.001$. (*D*) Comparison analysis of the pairwise combinations, control versus CreER *Stat3$^{f/f}$* and control versus CreER *Ube2n$^{f/f}$*, by IPA. (*E*) Venn diagram illustrating the number of cell death and survival genes, determined by pairwise comparison in IPA, with unique or overlapping association between the categories of inflammation and hematological development. (*F*) Heatmap of the 18 genes that overlap between cell death and survival, inflammation, and hematological development categories shown in *E*. Genes were clustered using Pearson distance metric and Ward's minimum variance method.

the overlap categories (Fig. 5 *E* and *F* and Fig. S5 *E* and *F*). Specifically, three of the seven genes that were up-regulated in *Stat3*-deficient LSKs according to RNA-seq showed significantly elevated expression in lin$^-$ cells by qPCR (Fig. 5 *E* and *F* and Fig. S5*E*). These include *Bmx* and *Clec4a2*, which encode regulators of TLR signaling, as well as *Itgb2*, encoding the integrin subunit CD11b, commonly associated with myeloid development (54–56). In addition, four of five genes in the overlap category that were induced in *Ube2n*-deficient LSKs by RNA-seq were confirmed to be up-regulated in lin$^-$ cells (Fig. 5 *E* and *F* and Fig. S5*F*). These include: *Ackr4*, encoding an atypical chemokine (scavenger) receptor; *Psen2*, encoding the Notch signaling mediator presenilin 2; *Mylk*, encoding myosin light-chain polypeptide kinase; and *Klrb1f*, encoding the lectin-like receptor CD161.

To further understand the impact of STAT3 and Ubc13 in LSKs, we performed two-way comparisons of differentially expressed genes using IPA core analysis. These studies revealed down-regulation of genes involved in maintaining blood cell quantities, hematopoiesis, and DNA repair in *Stat3*-deficient LSKs compared with control (Fig. S5*G* and Table S1). In contrast, *Ube2n*-deficient LSKs showed increased expression of genes involved in immune cell proliferation, and decreased expression of genes linked to apoptosis, inflammation, and cell death (Fig. S5*H* and Table S2). These results suggest STAT3 is important for hematopoietic survival and protection from DNA damage, while Ubc13 restrains cell proliferation or potentiates cell death or injury. Thus, our genome-wide transcriptional profiling studies indicate global yet distinct deregulation of gene expression upon *Stat3* or *Ube2n* deletion in LSKs, while concomitant removal of *Stat3* and *Ube2n* alleviated a majority of these aberrant gene-expression responses. Collectively, our data suggest hematopoietic-intrinsic STAT3 antiinflammatory activity is important for protecting stem and progenitor cells from the activation of intrinsic cell death, and inflammatory and inappropriate developmental gene-expression responses to preserve lineage-balanced hematopoiesis.

## Discussion

By employing three distinct model systems to target *Stat3* removal, we delineated an essential hematopoietic-intrinsic function for this key signaling mediator in HSPC maintenance, HSPC protection from DNA damage, suppression of myeloid-skewed blood cell production, and effective hematopoiesis. Our multipronged approach was necessary to rigorously evaluate STAT3 function in the hematopoietic system and avoid confounding issues due to gene deletion in nonhematopoietic tissues, or the contribution of peripheral inflammation driven by myeloid *Stat3*-deficiency to hematopoietic function. These questions arose because of the complexity of the Tie2 cre *Stat3*$^{f/f}$ mouse model, in which previous hematopoiesis studies have been performed (31, 36). Specifically, Tie2 cre *Stat3*$^{f/f}$ mice contain hematopoietic as well as endothelial *Stat3* deletion (47); endothelial *Stat3*-deficiency could impair critical hematopoietic niche function or provide a source of proinflammatory factors that injure HSPCs, affecting hematopoietic activity (37, 48, 49, 57, 58). In addition, Tie2 cre *Stat3*$^{f/f}$ mice develop systemic inflammation (35), which could influence hematopoiesis through a feedback mechanism to bone marrow HSPCs. Our analysis of HSPCs originating from LysM cre *Stat3*$^{f/f}$ animals indicates that peripheral inflammation driven by hyperactive *Stat3*-deficient myeloid cells is inadequate to damage STAT3-sufficient HSPCs. Furthermore, our use of CreER *Stat3*$^{f/f}$ mice and bone marrow transplantation allowed us to circumvent potential confounding issues due to *Stat3* deletion in nonhematopoietic populations. Collectively, our data reveal a critical hematopoietic-intrinsic role for STAT3 in maintaining lineage-balanced blood cell production.

STAT3 appears to be important at early developmental stages of hematopoiesis, including maintenance of the LSK CD150$^+$ CD48$^-$ subset, a population enriched for long-term repopulating HSCs (44). Moreover, we found *Stat3*-deficient HSPCs had characteristics of progenitors responding to inflammation, such as enhanced cell cycling and DNA damage. Thus, loss of blood cell-forming activity with hematopoietic-intrinsic *Stat3*-deficiency may be a consequence of fewer HSPCs, reduced HSPC function, or a combination of these factors. Nonetheless, inflammation hallmarks in *Stat3*-deficient HSPCs led us to hypothesize that the protective function for STAT3 in hematopoiesis may relate to its antiinflammatory activity, which is mediated through *Ube2n*/Ubc13 suppression (40). By removing Ubc13/*Ube2n* simultaneously from *Stat3*-deficient hematopoietic cells, lineage-balanced hematopoiesis and HSPC amounts became indistinguishable from *Stat3*- *Ube2n*-sufficient controls. Moreover, concomitant *Ube2n* and *Stat3* deletion reduced signs of DNA damage in HSPCs, and suppressed systemic inflammation found in *Stat3*-deficiency. These data indicate that a principal STAT3 antiinflammatory mechanism is mediated via Ubc13 modulation in vivo, and imply an epistatic relationship between STAT3 and Ubc13 in hematopoietic cells. In addition, our results suggest STAT3 antiinflammatory signaling is a critical means to preserve HSPCs and lineage-balanced hematopoiesis.

Nonetheless, key questions remain, as our model systems are unable to dissect the importance of intrinsic STAT3 antiinflammatory signaling within HSPCs from inflammation-independent STAT3 activity in progenitors, or from the impact of peripheral inflammatory mediators on the function of *Stat3*-deficient HSPCs. In fact, chimeric mice with hematopoietic *Stat3*-deficiency were unique among all cohorts in demonstrating elevated circulating myeloid cells and proinflammatory cytokines, suggesting HSPCs within these animals were distinctly exposed to inflammation. Thus, resolving the effects of intrinsic vs. peripheral proinflammatory signals in *Stat3*-deficient HSPCs, as well as inflammation-independent STAT3 target genes, will require novel approaches, such as genome-wide identification of STAT3-regulated genes in HSPCs under inflammatory and noninflammatory conditions, as well as animal models that separate HSPC-intrinsic STAT3 activity from STAT3 function in peripheral blood cell populations.

Although we observed lineage-balanced blood cell production upon hematopoietic-intrinsic *Ube2n* deletion, we cannot rule out a role for Ubc13 in hematopoiesis. We found a trend toward fewer LSK CD150$^+$ CD48$^-$ HPSCs as well as increased CMPs in the absence of Ubc13, which could suggest compensatory mechanisms enable lineage-balanced hematopoiesis upon *Ube2n* removal. Alterations in progenitor amounts are consistent with our transcriptional profiling, which indicated substantial gene expression responses mediated by Ubc13 in LSKs. Furthermore, prior reports have described roles for Ubc13 in B cell development and hematopoietic regulation (59, 60). Specifically, B cell-restricted (CD19 cre-directed) *Ube2n* deletion affected marginal zone B cells, peritoneal CD5$^+$ B-1 cells, and circulating amounts of immunoglobulins, yet did not alter B220 expression or splenic B220$^+$ B cell amounts (59). These data are consistent with our results, as our analyses were limited to circulating B220$^+$ B cells. In addition, animals with ubiquitous *Ube2n* deletion, mediated by the type I IFN-inducible MX cre transgene, showed dramatic hematopoietic failure, including multilineage immune cell deficiency (60). The MX cre model has potential to induce *Ube2n* deletion from both hematopoietic and stromal (e.g., HSC niche) populations and is accompanied by elevated type I IFN, which stimulates HSC proliferation (1). This model is notably distinct from our approach to direct hematopoietic-restricted *Ube2n* deletion, and suggests Ubc13 may have discrete functions in steady state and inflammatory conditions, or has important roles in hematopoietic-supportive niche populations. Interestingly, Ubc13 is involved in mediating DNA repair (61), although we did not detect notable DNA damage in HSPCs upon *Ube2n* deletion.

By comparing genome-wide transcriptional responses among control, *Stat3*-, *Ube2n*-, and *Stat3- Ube2n*-deficient LSKs, we identified 166 differentially regulated genes using a relatively stringent cut-off of FDR q value < 0.01. A subset of these differentially expressed genes is associated with inflammation, survival, and hematological development, suggesting a degree of overlap in regulation of these distinct cellular responses within HSPCs. Moreover, additional analysis indicated that survival and cellular injury pathways were distinctly controlled in *Stat3*- or *Ube2n*-deficient LSKs, as genes involved in blood cell maintenance, survival, and DNA repair were down-regulated in *Stat3*-deficient LSKs, while apoptosis and cell death genes showed reduced expression in *Ube2n*-deficient LSKs. Importantly, although STAT3 can restrain IFN signaling (62), we did not detect an obvious IFN gene signature in *Stat3*-deficient LSKs, suggesting *Stat3*-deficient HSPCs fail for reasons other than an intrinsically activated IFN response. The transcriptional profiling also detected a surprising similarity between control and *Stat3- Ube2n*-deficient LSKs, as significant differences were not detected between these populations using bioinformatic approaches. The extent of similarity between control and *Stat3- Ube2n*-deficient LSKs may reflect the fact that they are derived from mice lacking obvious signs of inflammation, as well as a unique complementation between the pathways deregulated by *Stat3*- or *Ube2n*-deficiency individually (e.g., survival or injury responses).

Validation of our RNA-seq data identified five genes that were previously associated with STAT3-dependent regulation—including *Bmx*, *Clec4a2*, *Ackr4*, *Psen2*, and *Mylk* (63)—suggesting these may be direct STAT3 targets. In addition, we confirmed increased *Itgb2* expression in *Stat3*-deficient HSPCs, which is consistent with myeloid-skewing in mice with hematopoietic *Stat3* deletion. Interestingly, three of the genes validated in *Ube2n*-deficiency (i.e., *Ackr4*, *Psen2*, and *Klrb1f*) show enriched expression or have major roles in lymphocytes and their development (64–69). Nonetheless, genome-wide RNA-seq or ChIP-sequencing (ChIP-seq) studies indicate STAT3 binds widely across the genome and exerts large-scale effects on transcription. Similar results have been reported for NF-κB–regulated genes, which can be induced upon Ubc13-mediated signaling (70–73). This makes it unlikely that deregulation of a single gene in *Stat3*-deficiency results in hematopoietic failure, or rescued expression of a single gene upon concomitant *Ube2n* removal salvages hematopoietic activity. Collectively, our transcriptional profiling and bioinformatic analyses are in agreement with the physiological responses we observed, and suggest a major outcome of STAT3 antiinflammatory signaling in the hematopoietic system is protection of HSPCs from injury and loss of viability.

STAT3 is often associated with deleterious responses and is frequently considered a proinflammatory signaling mediator, as well as a tumor-promoting factor. Hence approaches to mitigate STAT3 signaling have been pursued as cancer or antiinflammatory strategies (74–77). We suggest the picture is nuanced, however, particularly in the hematopoietic system. An important issue may be maintenance of balanced STAT3 function, a concept that is in line with the association of both human *STAT3* LOF and GOF mutations with immune disease (23, 26). In hematopoietic malignancy, blocking STAT3 may prove beneficial in selectively clearing tumor-sustaining stem cells by inducing their death, as STAT3 is critical for cell survival (30, 74). In inflammation conditions, however, therapeutic interference with STAT3 may exacerbate HSPC injury and result in unintended complications. Thus, targeting proinflammatory signaling mediators such as Ubc13 may be more effective methods to alleviate HSPC damage and bone marrow failure associated with chronic inflammation.

## Materials and Methods

**Animals.** Tie2 cre *Stat3*$^{f/f}$ [*Tg(Tek-cre)*$^{12Flv}$ *Stat3*$^{flox/flox}$] and LysM cre *Stat3*$^{f/f}$ [*Lyz2*$^{tm1(cre)Ifo}$ *Stat3*$^{flox/flox}$] mice were generated by crossing Tie2 cre or LysM cre strains with *Stat3*$^{f/f}$ mice (47, 78, 79), respectively. CreER *Stat3*$^{f/f}$, CreER *Ube2n*$^{f/f}$ and CreER *Stat3*$^{f/f}$ *Ube2n*$^{f/f}$ mice were produced by breeding CreER [*Gt(ROSA)26Sor*$^{tm1(cre/ERT2)Tyj}$] animals with *Stat3*$^{f/f}$ or *Ube2n*$^{f/f}$ mice (37, 50, 59). Age- and gender-matched *Stat3*-sufficient controls (*Stat3*$^{f/f}$) were included in all assays; controls include littermates and animals housed proximally. All strains were on the C57BL/6J background. Male and female mice aged 4–36 wk were used in experiments as follows: Tie2 cre *Stat3*$^{f/f}$ and *Stat3*-sufficient controls were used at ages 4–7 wk; LysM cre *Stat3*$^{f/f}$ and *Stat3*-sufficient controls were used at ages 12–18 wk (upon presentation of enterocolitis in LysM cre *Stat3*$^{f/f}$); CreER-containing strains used as donors in bone marrow transplantation were used at ages 6–8 wk. Congenic CD45.1$^+$ mice (B6.SJL-$^{Ptprca\ Pepcb/BoyJ}$) obtained from the Jackson Laboratories were utilized as recipients in bone marrow transplantation studies; mice were aged 6–10 wk. Final analyses of bone marrow recipients were performed 20 wk posttransplantation, when recipient mice were 34–38 wk old. Animals were housed in a specific pathogen-free facility. All experimental procedures were approved by the Institutional Animal Care and Use Committee at The University of Texas MD Anderson Cancer Center.

**Flow Cytometry and FACS.** To assess hematopoietic lineages, bone marrow and peripheral blood cell preparations, devoid of red blood cells, were stained with fluorescently labeled antibodies against CD45.1 (A20; BD Bioscience), CD45.2 (104; BD Bioscience), CD3 (CT-CD3; eBioscience), CD11b (M1/70; eBioscience), and CD45R/B220 (RA36B2; eBioscience). Samples were analyzed on an LSR Fortessa machine (BD Bioscience). For progenitor analysis, lin$^-$ bone marrow progenitors were enriched by magnetic bead separation using biotinylated rat anti-mouse antibodies against CD3, CD11b, Gr-1 (RB6-8C5; eBioscience), CD45R/B220, and Ter119 (Ter-119; eBioscience), followed by negative selection with anti-rat microbeads (Miltenyi Biotec). Enriched lin$^-$ cells were then stained with antibodies against CD34 (RAM34; eBioscience), FcγRII/III (2.4G2; eBioscience), CD45.2, Sca-1 (E13-161.7; eBioscience), CD45.1, c-Kit (2B8; eBioscience), CD48 (HM48-1; eBioscience), and CD150 (TC15-12F12.2; BioLegend) to label hematopoietic progenitors, and streptavidin-Pacific blue to label lin$^+$ cells. Cells were analyzed on an LSR Fortessa machine or isolated by FACs using FACSAria IIu sorter (BD Bioscience), as indicated in the text.

For HSPC cell cycle analysis and γH2AX staining, lin$^-$ bone marrow cells were enriched by magnetic bead separation and stained with fluorescently labeled antibodies to identify LSK (lin$^-$ Sca-1$^+$ c-Kit$^+$) and LSK CD150$^+$ CD48$^-$ populations. In cell cycle assays, cells were fixed and permeabilized using a commercial reagent (BD Bioscience), and then stained with the DNA dye Hoechst 33342 (Sigma-Aldrich) and fluorescently labeled antibody to the proliferation marker Ki67 (BD Bioscience). γH2AX staining was performed under similar conditions using fixed and permeabilized cells stained with an antibody to γH2AX (BD Bioscience). Cells were analyzed on an Influx or LSR Fortessa machine, respectively. Flow cytometry data were analyzed using FlowJo software.

**Bone Marrow and LSK CD150$^+$ CD48$^-$ Transplantation Assays.** Bone marrow cells were flushed from femurs and tibias of donor mice (6–8 wk of age) and stored in DMEM supplemented with 1% heat-inactivated FCS until transplantation. FACS-sorted LSK CD150$^+$ CD48$^-$ cells were isolated as described and stored in PBS until transplantation. Total bone marrow cells ($2 \times 10^6$) or FACS-sorted LSK CD150$^+$ CD48$^-$ cells (200) were transferred via tail vein injection (intravenously) into lethally irradiated (900 rad) CD45.1$^+$ congenic recipients (6–10 wk of age). For LSK CD150$^+$ CD48$^-$ cell transplantation, donor (CD45.2$^+$) cells were transferred with $10^5$ total bone marrow cells from the recipient strain (CD45.1$^+$), to provide a radioprotective dose of bone marrow. Peripheral blood was obtained at 4-wk intervals following LSK CD150$^+$ CD48$^-$ cell transplantation; cells were stained with antibodies and analyzed by flow cytometry to assess reconstitution efficiency. In total, bone marrow transplantation assays with CreER *Stat3*$^{f/f}$, CreER *Ube2n*$^{f/f}$, CreER *Stat3*$^{f/f}$ *Ube2n*$^{f/f}$, and control (*Stat3*$^{f/f}$) donor bone marrow, recipient mice were assessed for donor reconstitution at 8 wk posttransplantation; only animals with effective reconstitution (>80%) were used in subsequent assays. Chimeric mice were injected with tamoxifen (8 wk posttransplantation; 2 mg tamoxifen, every other day over a 1-wk interval) to induce gene deletion. Peripheral blood was obtained at 4-wk intervals following tamoxifen treatment, and analyzed for total and lineage reconstitution by antibody staining and flow cytometry. All animals were killed by 20 wk posttransplantation.

**RNA Isolation and qPCR.** Total RNA was extracted by TRIzol and reverse-transcribed with iScript (Bio-Rad); qPCR was performed with SYBR Green PCR Mix (Bio-Rad) and a sequence detector (Bio-Rad 5000). The expression of individual genes was calculated and normalized to 18s or GAPDH RNA. Data are presented as fold-change between the normalized test groups versus

normalized controls, as indicated in the figure legends. Gene-specific primers are listed in Table S5 or ref. 40.

**RNA-Seq.** Illumina compatible libraries were prepared using the Ovation RNA-Seq System V2 (Nugen) and the KAPA Hyper Library Preparation kit (KAPA) per the manufacturers' protocol. In brief, total RNA samples were assessed for quality and quantity using the Agilent Bioanalyzer RNA 6000 Pico Chip (Agilent Technologies). Two nanograms of total RNA were converted to double-stranded cDNA and amplified using Nugen's proprietary single primer isothermal (Ribo-SPIA) protocol. The double-stranded cDNA was then quantified using the Qubit DNA High Sensitivity Assay (ThermoFisher); 500 ng of each cDNA sample was fragmented to an average size of 200 bp using the Biorupter Pico Sonicator (Diagenode). The double-stranded cDNA fragments were end repaired, 5′-phosphorylated, and 3′-A tailed for ligation of the Y-shaped indexed adapters using the KAPA Hyper Library Prep kit (KAPA). Adapter ligated DNA fragments were amplified by two cycles of PCR, quantified by qPCR, and sequenced on the Illumina HiSeq4000 Sequencer using a 75-bp paired-end format.

**RNA-Seq Data Processing and Statistical Analysis.** The Genome Reference Consortium Mouse Build 38 (GRCm38/mm10) was used as the reference genome. TopHat2 was used for alignment of RNA-seq data, and Htseq-count was used to generate the read counts for each gene (80, 81). Bioconductor R package DESeq2 was used to normalize and analyze the RNA read counts matrix (82). Raw counts were normalized by gene geometric mean and sample median to adjust for sequencing depth. Negative binomial generalized linear models were used to test for differential expression. Wald tests were used for pairwise comparisons, and likelihood ratio tests were used as ANOVA-like tests, to test for the overall treatment effect. The Benjamini–Hochberg method was applied to adjust for multiple comparisons (83). Genes with FDR q value $< 0.01$, identified by likelihood ratio tests, were considered significant. Genes with FDR q value $< 0.05$ by Wald tests and fold-change larger than $\pm 2$ were identified as significant in pairwise comparisons. Two-way clustering heatmaps, using Pearson distance metric and Ward's minimum variance method, were used to illustrate the expression profile of the identified genes. Data were analyzed by IPA (Qiagen; https://www.qiagenbioinformatics.com/products/ingenuity-pathway-analysis) (84). IPA was performed for the 166 significant genes (FDR q value $< 0.01$) identified by a likelihood ratio test. The IPA analysis uses Fisher's exact test to generate *P* values for curated gene sets separately grouped by canonical pathways, upstream regulators, and biological functions and diseases. IPA core analysis was used to identify disease pathways differentially regulated among genes that show significantly different expression in two-way comparisons. Venn diagrams were generated by Bioinformatics and Evolutionary Genomics (bioinformatics.psb.ugent.be/webtools/Venn/).

**Multiplex Cytokine Analysis.** Serum samples were analyzed using the Luminex Multiplexed Bead Array kit (ProcartaPlex-20 Plex; eBioscience) for 20 different cytokines and chemokines (IL-6, IFN-α, IFN-γ, TNF-α, IL-1β, IL-1α, IL-10, IL-17A, IL-12, IL-23, G-CSF, GM-CSF, M-CSF, LIF, VEGFα, IP10, MIP2, KC, MCP1, and MCP3) according to the manufacturer's instructions. Median fluorescence intensities were collected on a Luminex-100 instrument (Luminex Corp) using Bio-Plex Manager 6.1 (Bio-Rad) software. Cytokine concentrations were determined from the appropriate standard curves of known concentrations of recombinant mouse cytokines and chemokines to convert fluorescence units to concentrations (pg/mL). Each sample was run in duplicate and the mean of the duplicate was used to calculate the measured concentration.

**Alkaline Comet Assays.** For alkaline comet assays, $1 \times 10^4$ FACS-purified LSKs were suspended in 10 μL ice-cold PBS, and mixed with 100 μL of prewarmed (37 °C) 0.75% low melting-point agarose. Next, 50 μL of the mixture was dropped on a fully frosted slide precosted with 0.5% agarose gel. After solidification, slides were immersed in precooled lysis solution (Trevigen) at 4 °C and incubated in the dark for 1 h. Excess lysis buffer was drained from the slides, and slides were immersed in freshly prepared and precooled alkaline DNA unwinding solution (200 mM NaOH, 1 mM EDTA, pH $> 13$) for 30 min at 4 °C in the dark. Electrophoresis was performed using 18 volts for 30 min at 4 °C in the dark. Following electrophoresis, slides were gently immersed twice into $ddH_2O$ for 5 min each and fixed in 70% ethanol for 5 min. After air drying, DNA was stained with SYBR Gold (Trevigen) solution for 30 min at room temperature. Images were captured by a Nikon 80i fluorescent microscope and analyzed using OpenComet software.

**Immunoblotting.** Whole-cell lysates were subjected to SDS/PAGE and immunoblotting, using antibodies to STAT3 (c-20; Santa Cruz Biotechnology), Ubc13 (#371100; Invitrogen), and RAN (c-20; Santa Cruz Biotechnology) as described previously (40).

**Statistical Analysis.** Data are presented as mean ± SEM. The statistical significance between two groups was calculated by a two-tailed *t* test. For multiple groups, significance was evaluated by one-way or two-way ANOVA with Tukey multiple comparisons. Graphpad Prism 5 software was used for each type of analysis. Statistical analyses of RNA-seq data are described in *RNA-Seq Data Processing and Statistical Analysis*, above.

**ACKNOWLEDGMENTS.** We thank Dr. Katherine King for critical review of this manuscript; Drs. Peggy Goodell and Sharon Dent for scientific advice; Anna Zal and Dr. Tomasz Zal for assistance; members of the flow cytometry core laboratory and the DNA sequencing core labortory at MD Anderson for technical help; and Dr. Luis Vence for assistance with cytokine multiplex analyses. This work was supported by NIH National Institute of Allergy and Infectious Diseases Grants R01AI057555 (to S.-C.S.) and R01AI109294 (to S.S.W.); a grant from the MD Anderson Center for Stem Cell and Developmental Biology (to S.S.W.); a grant from the MD Anderson Center for Inflammation and Cancer (to S.S.W. and H.Z.); and Research Training Award from the Cancer Prevention and Research Institute of Texas CPRIT RP170067 (to T.T.C.). The MD Anderson Center for Cancer Epigenetics provided a pilot award for RNA-seq experiments. Core facilities at MD Anderson, including the Sequencing and Microarray Core and the Flow Cytometry Core, were supported by the institutional Core Grant P30CA16672 from the NIH National Cancer Institute.

1. Essers MA, et al. (2009) IFNalpha activates dormant haematopoietic stem cells in vivo. *Nature* 458:904–908.
2. Baldridge MT, King KY, Boles NC, Weksberg DC, Goodell MA (2010) Quiescent haematopoietic stem cells are activated by IFN-gamma in response to chronic infection. *Nature* 465:793–797.
3. Matatall KA, Shen CC, Challen GA, King KY (2014) Type II interferon promotes differentiation of myeloid-biased hematopoietic stem cells. *Stem Cells* 32:3023–3030.
4. Pietras EM, et al. (2014) Re-entry into quiescence protects hematopoietic stem cells from the killing effect of chronic exposure to type I interferons. *J Exp Med* 211: 245–262.
5. Pietras EM, et al. (2016) Chronic interleukin-1 exposure drives haematopoietic stem cells towards precocious myeloid differentiation at the expense of self-renewal. *Nat Cell Biol* 18:607–618.
6. Esplin BL, et al. (2011) Chronic exposure to a TLR ligand injures hematopoietic stem cells. *J Immunol* 186:5367–5375.
7. Matatall KA, et al. (2016) Chronic infection depletes hematopoietic stem cells through stress-induced terminal differentiation. *Cell Rep* 17:2584–2595.
8. Walter D, et al. (2015) Exit from dormancy provokes DNA-damage-induced attrition in haematopoietic stem cells. *Nature* 520:549–552.
9. Zhang H, et al. (2016) Sepsis induces hematopoietic stem cell exhaustion and myelosuppression through distinct contributions of TRIF and MYD88. *Stem Cell Reports* 6: 940–956.
10. Starczynowski DT, et al. (2010) Identification of miR-145 and miR-146a as mediators of the 5q- syndrome phenotype. *Nat Med* 16:49–58.
11. Starczynowski DT, Karsan A (2010) Innate immune signaling in the myelodysplastic syndromes. *Hematol Oncol Clin North Am* 24:343–359.
12. Wei Y, et al. (2013) Toll-like receptor alterations in myelodysplastic syndrome. *Leukemia* 27:1832–1840.
13. Wei Y, et al. (2013) Global H3K4me3 genome mapping reveals alterations of innate immunity signaling and overexpression of JMJD3 in human myelodysplastic syndrome CD34+ cells. *Leukemia* 27:2177–2186.
14. Rhyasen GW, et al. (2013) Targeting IRAK1 as a therapeutic approach for myelodysplastic syndrome. *Cancer Cell* 24:90–104.
15. Fang J, et al. (2014) Myeloid malignancies with chromosome 5q deletions acquire a dependency on an intrachromosomal NF-κB gene network. *Cell Rep* 8:1328–1338.
16. Gañán-Gómez I, et al. (2015) Deregulation of innate immune and inflammatory signaling in myelodysplastic syndromes. *Leukemia* 29:1458–1469.
17. Waight JD, Hu Q, Miller A, Liu S, Abrams SI (2011) Tumor-derived G-CSF facilitates neoplastic growth through a granulocytic myeloid-derived suppressor cell-dependent mechanism. *PLoS One* 6:e27690.
18. Waight JD, et al. (2013) Myeloid-derived suppressor cell development is regulated by a STAT/IRF-8 axis. *J Clin Invest* 123:4464–4478.
19. Casbon AJ, et al. (2015) Invasive breast cancer reprograms early myeloid differentiation in the bone marrow to generate immunosuppressive neutrophils. *Proc Natl Acad Sci USA* 112:E566–E575.
20. Kane A, et al. (2014) STAT3 is a central regulator of lymphocyte differentiation and function. *Curr Opin Immunol* 28:49–57.
21. Wake MS, Watson CJ (2015) STAT3 the oncogene—Still eluding therapy? *FEBS J* 282: 2600–2611.
22. Hillmer EJ, Zhang H, Li HS, Watowich SS (2016) STAT3 signaling in immunity. *Cytokine Growth Factor Rev* 31:1–15.

23. Holland SM, et al. (2007) STAT3 mutations in the hyper-IgE syndrome. *N Engl J Med* 357:1608–1619.
24. Minegishi Y, et al. (2007) Dominant-negative mutations in the DNA-binding domain of STAT3 cause hyper-IgE syndrome. *Nature* 448:1058–1062.
25. Milner JD, et al. (2008) Impaired T(H)17 cell differentiation in subjects with autosomal dominant hyper-IgE syndrome. *Nature* 452:773–776.
26. Milner JD, et al. (2015) Early-onset lymphoproliferation and autoimmunity caused by germline STAT3 gain-of-function mutations. *Blood* 125:591–599.
27. Yu H, Lee H, Herrmann A, Buettner R, Jove R (2014) Revisiting STAT3 signalling in cancer: New and unexpected biological functions. *Nat Rev Cancer* 14:736–746.
28. Ferguson SD, Srinivasan VM, Heimberger AB (2015) The role of STAT3 in tumor-mediated immune suppression. *J Neurooncol* 123:385–394.
29. Furqan M, et al. (2013) STAT inhibitors for cancer therapy. *J Hematol Oncol* 6:90.
30. Munoz J, Dhillon N, Janku F, Watowich SS, Hong DS (2014) STAT3 inhibitors: Finding a home in lymphoma and leukemia. *Oncologist* 19:536–544.
31. Zhang H, et al. (2010) STAT3 controls myeloid progenitor growth during emergency granulopoiesis. *Blood* 116:2462–2471.
32. Esashi E, et al. (2008) The signal transducer STAT5 inhibits plasmacytoid dendritic cell development by suppressing transcription factor IRF8. *Immunity* 28:509–520.
33. Oh IH, Eaves CJ (2002) Overexpression of a dominant negative form of STAT3 selectively impairs hematopoietic stem cell activity. *Oncogene* 21:4778–4787.
34. Chung YJ, et al. (2006) Unique effects of Stat3 on the early phase of hematopoietic stem cell regeneration. *Blood* 108:1208–1215.
35. Welte T, et al. (2003) STAT3 deletion during hematopoiesis causes Crohn's disease-like pathogenesis and lethality: A critical role of STAT3 in innate immunity. *Proc Natl Acad Sci USA* 100:1879–1884.
36. Mantel C, et al. (2012) Mouse hematopoietic cell-targeted STAT3 deletion: Stem/progenitor cell defects, mitochondrial dysfunction, ROS overproduction, and a rapid aging-like phenotype. *Blood* 120:2589–2599.
37. Takeda K, et al. (1999) Enhanced Th1 activity and development of chronic enterocolitis in mice devoid of Stat3 in macrophages and neutrophils. *Immunity* 10:39–49.
38. El Kasmi KC, et al. (2006) General nature of the STAT3-activated anti-inflammatory response. *J Immunol* 177:7880–7888.
39. O'Shea JJ, Murray PJ (2008) Cytokine signaling modules in inflammatory responses. *Immunity* 28:477–487.
40. Zhang H, et al. (2014) STAT3 restrains RANK- and TLR4-mediated signalling by suppressing expression of the E2 ubiquitin-conjugating enzyme Ubc13. *Nat Commun* 5: 5798.
41. Panopoulos AD, et al. (2006) STAT3 governs distinct pathways in emergency granulopoiesis and mature neutrophils. *Blood* 108:3682–3690.
42. Heimall J, Freeman A, Holland SM (2010) Pathogenesis of hyper IgE syndrome. *Clin Rev Allergy Immunol* 38:32–38.
43. Deng L, et al. (2000) Activation of the IkappaB kinase complex by TRAF6 requires a dimeric ubiquitin-conjugating enzyme complex and a unique polyubiquitin chain. *Cell* 103:351–361.
44. Kiel MJ, et al. (2005) SLAM family receptors distinguish hematopoietic stem and progenitor cells and reveal endothelial niches for stem cells. *Cell* 121:1109–1121.
45. Orford KW, Scadden DT (2008) Deconstructing stem cell self-renewal: Genetic insights into cell-cycle regulation. *Nat Rev Genet* 9:115–128.
46. Wilson A, et al. (2008) Hematopoietic stem cells reversibly switch from dormancy to self-renewal during homeostasis and repair. *Cell* 135:1118–1129.
47. Koni PA, et al. (2001) Conditional vascular cell adhesion molecule 1 deletion in mice: Impaired lymphocyte migration to bone marrow. *J Exp Med* 193:741–754.
48. Ding L, Saunders TL, Enikolopov G, Morrison SJ (2012) Endothelial and perivascular cells maintain haematopoietic stem cells. *Nature* 481:457–462.
49. Ding L, Morrison SJ (2013) Haematopoietic stem cells and early lymphoid progenitors occupy distinct bone marrow niches. *Nature* 495:231–235.
50. Ventura A, et al. (2007) Restoration of p53 function leads to tumour regression in vivo. *Nature* 445:661–665.
51. Nagai Y, et al. (2006) Toll-like receptors on hematopoietic progenitor cells stimulate innate immune system replenishment. *Immunity* 24:801–812.
52. Zhao JL, et al. (2014) Conversion of danger signals into cytokine signals by hematopoietic stem and progenitor cells for regulation of stress-induced hematopoiesis. *Cell Stem Cell* 14:445–459.
53. Takizawa H, et al. (2017) Pathogen-induced TLR4-TRIF innate immune signaling in hematopoietic stem cells promotes proliferation but reduces competitive fitness. *Cell Stem Cell* 21:225–240.e5.
54. Kanazawa N, et al. (2002) DCIR acts as an inhibitory receptor depending on its immunoreceptor tyrosine-based inhibitory motif. *J Invest Dermatol* 118:261–266.
55. Palmer CD, et al. (2008) Bmx tyrosine kinase regulates TLR4-induced IL-6 production in human macrophages independently of p38 MAPK and NFkappB activity. *Blood* 111: 1781–1788.
56. Fujikado N, et al. (2008) Dcir deficiency causes development of autoimmune diseases in mice due to excess expansion of dendritic cells. *Nat Med* 14:176–180.
57. Kano A, et al. (2003) Endothelial cells require STAT3 for protection against endotoxin-induced inflammation. *J Exp Med* 198:1517–1525.
58. Boettcher S, et al. (2014) Endothelial cells translate pathogen signals into G-CSF-driven emergency granulopoiesis. *Blood* 124:1393–1403.
59. Yamamoto M, et al. (2006) Key function for the Ubc13 E2 ubiquitin-conjugating enzyme in immune receptor signaling. *Nat Immunol* 7:962–970.
60. Wu X, Yamamoto M, Akira S, Sun SC (2009) Regulation of hematopoiesis by the K63-specific ubiquitin-conjugating enzyme Ubc13. *Proc Natl Acad Sci USA* 106:20836–20841.
61. Kolas NK, et al. (2007) Orchestration of the DNA-damage response by the RNF8 ubiquitin ligase. *Science* 318:1637–1640.
62. Costa-Pereira AP, et al. (2002) Mutational switch of an IL-6 response to an interferon-gamma-like response. *Proc Natl Acad Sci USA* 99:8043–8047.
63. Vallania F, et al. (2009) Genome-wide discovery of functional transcription factor binding sites by comparative genomics: The case of Stat3. *Proc Natl Acad Sci USA* 106: 5117–5122.
64. Iizuka K, Naidenko OV, Plougastel BF, Fremont DH, Yokoyama WM (2003) Genetically linked C-type lectin-related ligands for the NKRP1 family of natural killer cell receptors. *Nat Immunol* 4:801–807.
65. Laky K, Fowlkes BJ (2007) Presenilins regulate alphabeta T cell development by modulating TCR signaling. *J Exp Med* 204:2115–2129.
66. Heinzel K, Benz C, Bleul CC (2007) A silent chemokine receptor regulates steady-state leukocyte homing in vivo. *Proc Natl Acad Sci USA* 104:8421–8426.
67. Yagi T, et al. (2008) Defective signal transduction in B lymphocytes lacking presenilin proteins. *Proc Natl Acad Sci USA* 105:979–984.
68. Comerford I, et al. (2010) The atypical chemokine receptor CCX-CKR scavenges homeostatic chemokines in circulation and tissues and suppresses Th17 responses. *Blood* 116:4130–4140.
69. Bunting MD, et al. (2013) CCX-CKR deficiency alters thymic stroma impairing thymocyte development and promoting autoimmunity. *Blood* 121:118–128.
70. Lim CA, et al. (2007) Genome-wide mapping of RELA(p65) binding identifies E2F1 as a transcriptional activator recruited by NF-kappaB upon TLR4 activation. *Mol Cell* 27: 622–635.
71. Durant L, et al. (2010) Diverse targets of the transcription factor STAT3 contribute to T cell pathogenicity and homeostasis. *Immunity* 32:605–615.
72. Hutchins AP, Poulain S, Miranda-Saavedra D (2012) Genome-wide analysis of STAT3 binding in vivo predicts effectors of the anti-inflammatory response in macrophages. *Blood* 119:e110–e119.
73. Hutchins AP, Takahashi Y, Miranda-Saavedra D (2015) Genomic analysis of LPS-stimulated myeloid cells identifies a common pro-inflammatory response but divergent IL-10 anti-inflammatory responses. *Sci Rep* 5:9100.
74. Yu H, Pardoll D, Jove R (2009) STATs in cancer inflammation and immunity: A leading role for STAT3. *Nat Rev Cancer* 9:798–809.
75. Zhang S, Hwaiz R, Luo L, Herwald H, Thorlacius H (2015) STAT3-dependent CXC chemokine formation and neutrophil migration in streptococcal M1 protein-induced acute lung inflammation. *Am J Physiol Lung Cell Mol Physiol* 308:L1159–L1167.
76. Gavino AC, Nahmod K, Bharadwaj U, Makedonas G, Tweardy DJ (2016) STAT3 inhibition prevents lung inflammation, remodeling, and accumulation of Th2 and Th17 cells in a murine asthma model. *Allergy* 71:1684–1692.
77. Ahmad SF, et al. (2017) STA-21, a STAT-3 inhibitor, attenuates the development and progression of inflammation in collagen antibody-induced arthritis. *Immunobiology* 222:206–217.
78. Takeda K, et al. (1998) Stat3 activation is responsible for IL-6-dependent T cell proliferation through preventing apoptosis: Generation and characterization of T cell-specific Stat3-deficient mice. *J Immunol* 161:4652–4660.
79. Clausen BE, Burkhardt C, Reith W, Renkawitz R, Förster I (1999) Conditional gene targeting in macrophages and granulocytes using LysMcre mice. *Transgenic Res* 8: 265–277.
80. Kim D, et al. (2013) TopHat2: Accurate alignment of transcriptomes in the presence of insertions, deletions and gene fusions. *Genome Biol* 14:R36.
81. Anders S, Pyl PT, Huber W (2015) HTSeq—A Python framework to work with high-throughput sequencing data. *Bioinformatics* 31:166–169.
82. Love MI, Huber W, Anders S (2014) Moderated estimation of fold change and dispersion for RNA-seq data with DESeq2. *Genome Biol* 15:550.
83. Benjamini Y, Hochberg Y (1995) Controlling the false discovery rate: A practical and powerful approach to multiple testing. *J R Stat Soc Series B (Methodol)* 57:289–300.
84. Krämer A, Green J, Pollard J, Jr, Tugendreich S (2014) Causal analysis approaches in ingenuity pathway analysis. *Bioinformatics* 30:523–530.